CHEMISTRY
A EUROPEAN JOURNAL

COMMUNICATION

DOI: 10.1002/chem.201302633

Molar-Ratio-Dependent Supramolecular Isomerism: Ag^{I} Coordination Polymers with Bis(cyanobenzyl)sulfides

Eunji Lee, Ja-Yeon Kim, Shim Sung Lee,* and Ki-Min Park*[a]

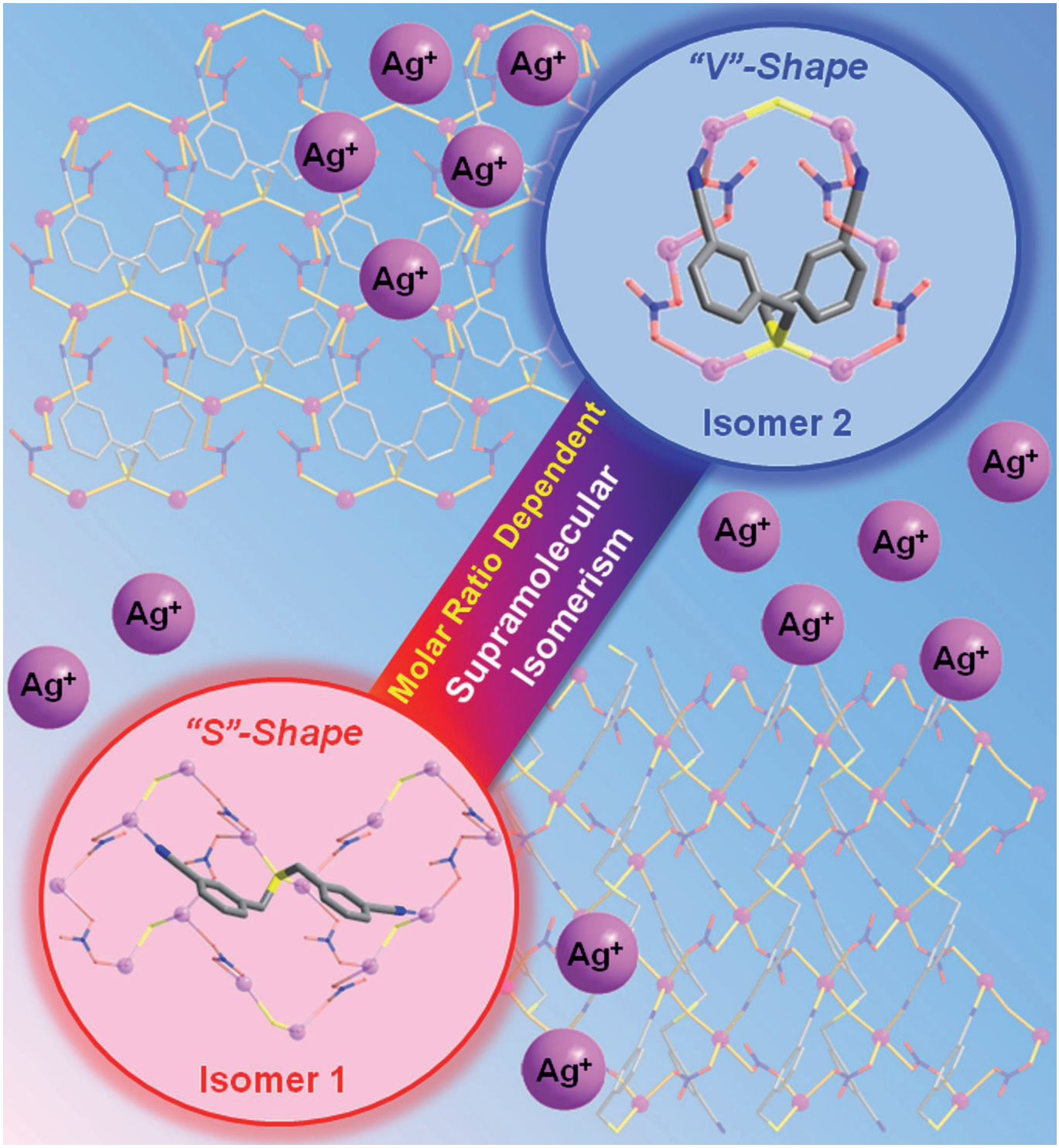

Supramolecular isomerism has received increasing attention in the area of molecular and crystal engineering, since Zaworotko first coined the term "supramolecular isomers".[1] Such isomers correspond to different supramolecular structures constructed from the same molecular building blocks, giving rise to structural isomerism at the supramolecular level—a range of papers concerned with supramolecular isomerism have now appeared in the literature.[2–9] In this context, refining the synthetic procedures used to produce supramolecular isomers is important, since it provides an opportunity for gaining a better understanding of the factors that influence the formation of individual isomer structures.

There have been a number of studies focused on understanding the factors leading to supramolecular isomerism. Until now, factors such as temperature,[3] choice of solvent,[4] the presence of a template[5] or guest,[6] pH,[7] catenation[8] or concentration[9] have all been shown to affect the self-assembly of particular supramolecular isomers.

Over recent years our group has investigated the use of ligands incorporating sulfur donors in conjunction with aromatic backbone unit on the structural diversity often observed in the resulting discrete and infinite supramolecular product obtained from such systems.[10] In the present study the three regioisomers of bis(cyanobenzyl)sulfide (*o*-**L**, *m*-**L**, and *p*-**L**) were chosen as organic building blocks for assembly reactions with thiaphilic $AgNO_3$.

These ligands are somewhat flexible due to free rotation around the C–S and C–C bonds, and this appeared likely to induce structural diversity across their respective com-

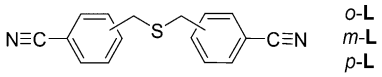

plexes.[11] For example, on coordination of a soft metal ion to their sulfur donors, *o*-**L** and *p*-**L** might be expected to favour metallocyclic and linear products, respectively (when the coordination vectors associated with the positions of the terminal cyano groups are considered). In contrast, reflecting its intermediate nature of *m*-**L** between *o*-**L** and *p*-**L**, it is difficult to predict the likely coordination behaviour. For this ligand system we have investigated whether minor factors such as the molar ratio of the reactants (that is, the metal-to-ligand ratio) might be employed to control the nature of the resulting complex type. Based on this assumption, we performed a systematic series of experiments in which the effect of changing the molar ratio of the metal salt to ligand in the syntheses of $AgNO_3$ complexes of *m*-**L** was investigated; comparative studies for *o*-**L** and *p*-**L** were also carried out.

Overall we have been successful in isolating four silver(I) coordination polymers (**1**–**4**) with different topologies from the reaction of $AgNO_3$ with *o*-**L**, *m*-**L** and *p*-**L**. Indeed, an intriguing feature of the results is the observation of molar-ratio-dependent supramolecular isomerism (or conformational polymorphism) in the formation of the 2D coordination polymers obtained with *m*-**L** (isomers **1** and **2**, Scheme 1). The conformational difference adopted by *m*-**L** has been probed by single-crystal X-ray analysis. Powder X-ray diffraction (PXRD) analysis has also been applied to monitor the observed molar-ratio-dependent supramolecular isomerism. To the best of our knowledge, supramolecular isomerism of this type has not been reported previously for network complexes.

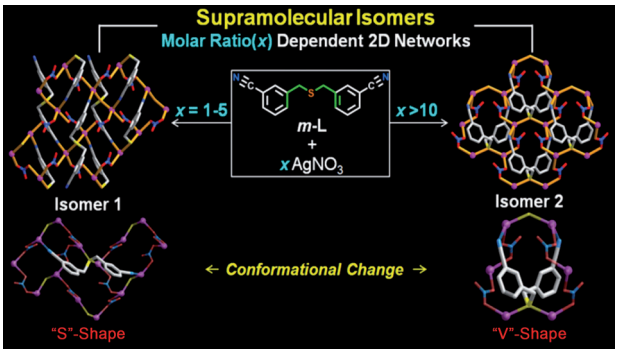

Scheme 1. Molar-ratio-dependent supramolecular isomers **1** and **2** showing the conformational differences of *m*-**L** in each.

The ligands *o*-**L**, *m*-**L** and *p*-**L** were synthesised by the reaction of sodium sulfide and the corresponding bromomethyl benzonitrile derivative in methanol–water (7:3 v/v) (Supporting Information); the synthesis of *p*-**L** from the reaction of *p*-cyanobenzyl mercaptan and *p*-cyanobenzyl chloride has also been previously reported by Barkenbus et al.[12]

For the synthesis of **1**–**4**, the concentration of $AgNO_3$ was varied relative to the ligand concentration in order to examine the effect of reactant molar ratio on the nature of the resulting complexes. Notably, this approach enabled us to isolate the supramolecular isomers of **1** and **2** incorporating *m*-**L** (Scheme 1). The individual isomer structures and connectivity patterns were found to be reflected by the ligand conformations as depicted in Scheme 1. Under identical reaction conditions to the above, *o*-**L** and *p*-**L** solely yielded the respective products **3** and **4**; that is, no molar-ratio dependency was observed in either case.

Preparation and structural comparison of supramolecular isomers (1 and 2): Direct mixing of a solution of *m*-**L** in dichloromethane with one equivalent of $AgNO_3$ in methanol and allowing the solution to evaporate at room temperature afforded **1** as a colourless crystalline product. As mentioned above, when a large excess of $AgNO_3$ (above ten equiva-

[a] E. Lee, J.-Y. Kim, S. S. Lee, K.-M. Park
Department of Chemistry and Research Institute of Natural Science
Gyeongsang National University, Jinju 660-701 (Republic of Korea)
E-mail: sslee@gsnu.ac.kr
kmpark@gnu.ac.kr

Supporting information for this article is available on the WWW under http://dx.doi.org/10.1002/chem.201302633.

lents) was reacted with *m*-**L**, **2** was obtained as colourless crystals. Single-crystal X-ray analysis confirmed that **1** and **2** are supramolecular isomers with the composition $[Ag_2(m\text{-}\mathbf{L})(NO_3)_2]_n$. Both feature 2D polymeric arrangements (Figures 1 and 2). Comparison of the PXRD patterns for the synthesised products with the simulated patterns for isomers **1** and **2** confirmed that the isolated samples were phase pure (see Figure 3, below).

Isomer **1** crystallised in the monoclinic space group $P2_1$ with $Z=2$. The asymmetric unit contains one molecule of *m*-**L**, two Ag atoms, and two NO_3^- moieties. The two Ag atoms (Ag1 and Ag2, Figure 1a) show similar coordination environments. Each Ag centre is four-coordinate, being bound to one cyano nitrogen atom from one *m*-**L**, one sulfur atom from an adjacent *m*-**L**, and two monodentate NO_3^- ions. The coordination geometry around each Ag atom in **1** is distorted tetrahedral, with the "tetrahedral" angles falling in the range 91.8(1)–127.1(1)° for Ag1 and 88.8(1)–123.7(1)° for Ag2. Isomer **2** crystallised in the monoclinic space group $C2/c$ with $Z=4$. The asymmetric unit contains a half-molecule of *m*-**L**, one Ag atom, and one NO_3^- ion, since *m*-**L** is located on a two-fold rotation axis. The Ag atom in this isomer is also four-coordinate and its local coordination environment (85.2(1)–133.1(1)°) is similar to that of the Ag atom in isomer **1** (Figure 2a).

In isomer **1**, Ag atoms are linked by μ_2-NO_3^- to form a 1D zigzag backbone, with further cross-linking by *m*-**L** (through Ag–S and Ag–N bonds) to form a 2D layer. Isomer **1** has a (6,3) net topology, in which Ag atoms provide the three-connected nodes to yield a herringbone pattern with a rectangular window as a single block unit (Figure 1b and c). That is, the single block unit of **1** is a simple 20-membered metallocycle $\{Ag_6(NO_2)_4S_2\}$, in which six Ag atoms are linked by four μ_2-NO_3^- units and two sulfur donors. The association of the single block unit in the herringbone arrangement generates the neutral puckered 2D network **1**. Similar to isomer **1**, the 2D network of isomer **2** is made up of 1D $(Ag{-}NO_3)_n$ zigzag backbones. These inorganic backbones are further cross-linked by *m*-**L** units by means of Ag–S and Ag–N bonds to give a distorted honeycomb-like 2D network. Isomer **2** also has a (6,3) net topology and Ag atoms provide the three-connected nodes (Figure 2b,c). So, in general, the connectivity pattern and the composition of the single block unit in **2** is almost identical to that in **1**.

The most striking difference between the two isomers lies in the conformation of *m*-**L**, which acts as a tridentate ligand in each case. For example, *m*-**L** in **1** is fully "stretched" and its two cyano groups are oriented away from each other to form an "S"-shaped configuration (Figure 1d). So, the three consecutive block units in **1** contain one *m*-**L** molecule with a *trans–gauche–gauche–trans* arrangement through two Ag-N and one Ag–S bonds. A single block unit in isomer **2** holds one *m*-**L** molecule with a "V"-shape and a *gauche–gauche–gauche–gauche* arrangement through two Ag–N bonds and one Ag–S bond (Figure 2d). Accordingly, the length of *m*-**L** (N1···N1C 7.46 Å) in **2** is much shorter than that in isomer **1** (N1···N2 12.49 Å).

In the packing structure, the 2D sheets in **1** are stacked with weak C–H···O hydrogen bonds (2.55 and 2.43 Å, dashed lines in Figure 1e) with interlayer separation of half the *a*-axial length (10.123 Å). The structure of **2** (Figure 2b)

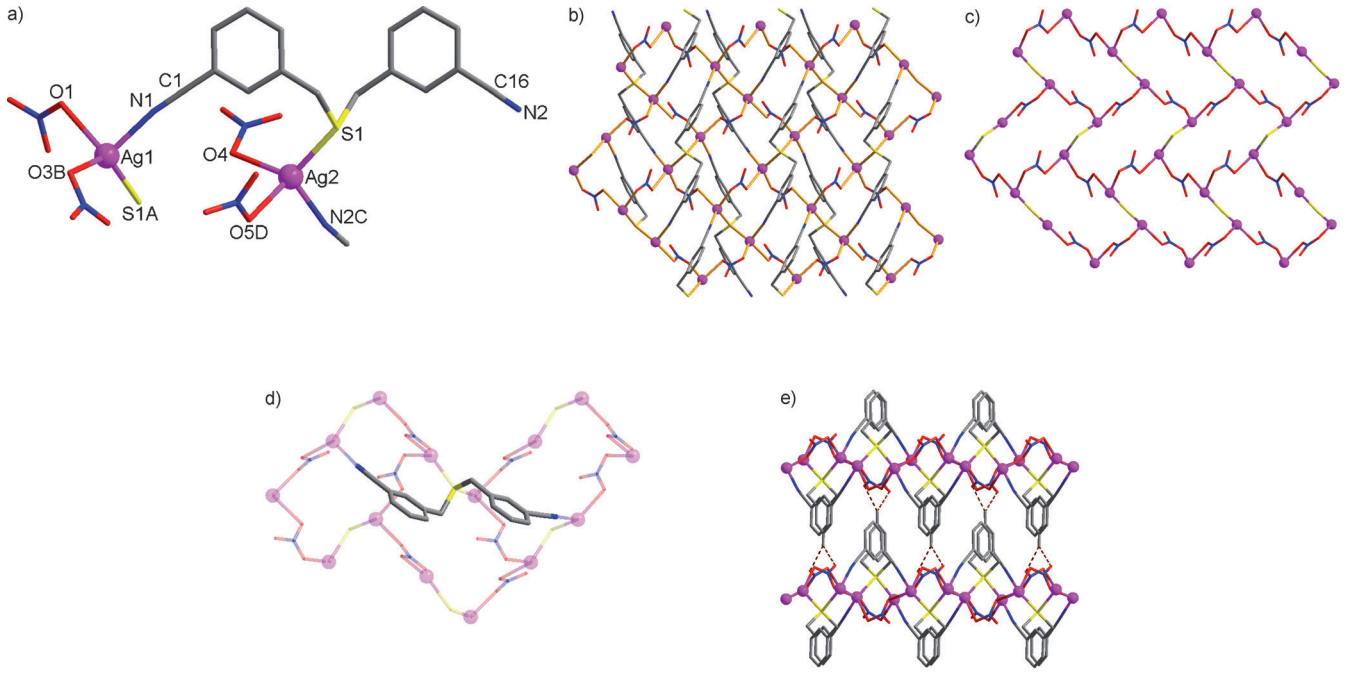

Figure 1. Crystal structure of isomer **1**, $[Ag_2(m\text{-}\mathbf{L})(NO_3)_2]_n$: a) basic coordination unit, b) 2D layered network, c) herringbone pattern (ligands are omitted except for sulfur atoms), d) "S"-shape ligand conformation showing the *trans-gauche-gauche-trans* arrangement in three consecutive block units, and e) packing arrangement showing interlayer C–H···O hydrogen bonds.

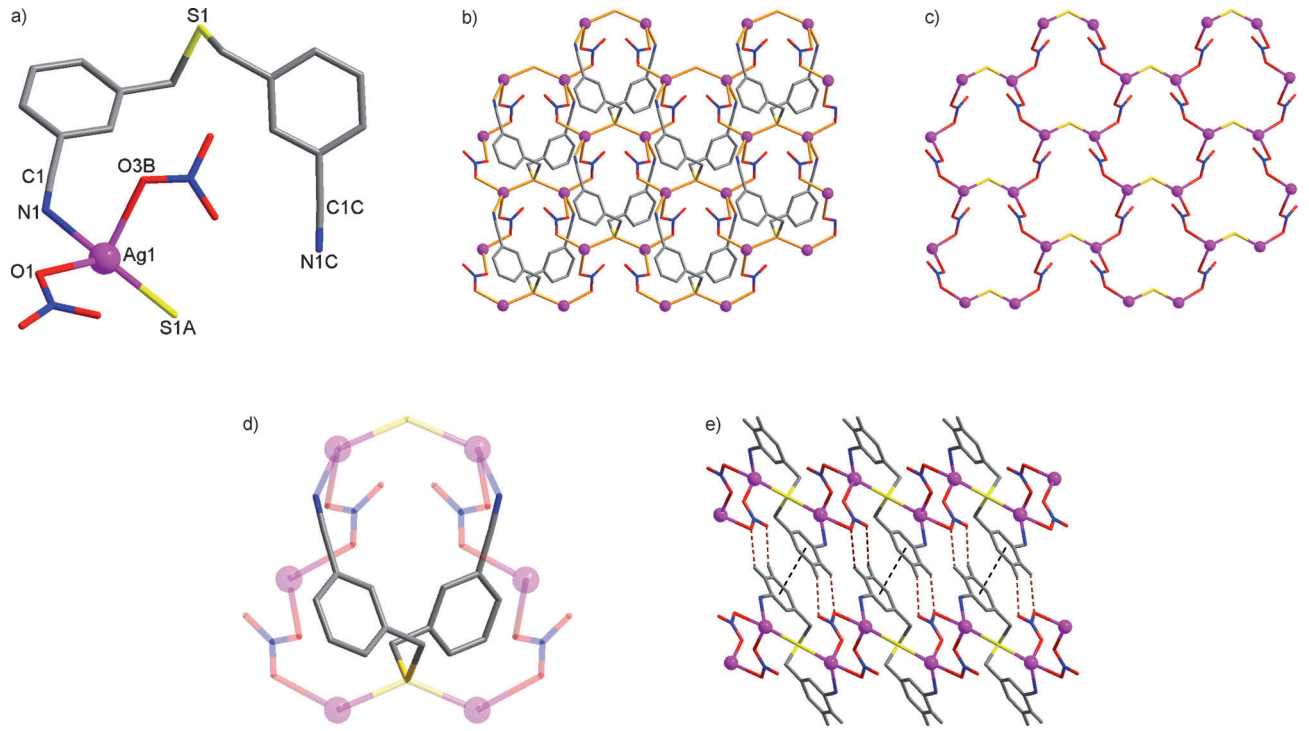

Figure 2. Crystal structure of isomer **2**, $[Ag_2(m\text{-}\mathbf{L})(NO_3)_2]_n$: a) basic coordination unit, b) 2D layered network, c) distorted honeycomb pattern (ligands are omitted except for sulfur atoms), d) "V"-shape ligand conformation showing the *gauche–gauche–gauche–gauche* arrangement in a single block unit, and e) packing arrangement showing interlayer C–H···O hydrogen-bonds and π–π interactions.

is also reinforced by interlayer interactions by weak C–H···O hydrogen bonds (2.60 and 2.63 Å, dashed lines in Figure 2e) as well as by π···π stacking interactions (centroid···centroid 3.75 Å) with the interlayer separation half of the *c*-axial length (9.145 Å).

The different structures observed for **1** and **2** are reflected in the conformational differences of the *m*-**L** ligand in each product. To the best of our knowledge, this is the first example of supramolecular isomers based on conformational ligand changes that are induced by a molar-ratio variation of the reactants employed for their synthesis.

PXRD study of supramolecular isomers (1 and 2): Our systematic studies in which the reactant molar ratios were varied to give supramolecular isomerism were monitored by the determination of consecutive PXRD patterns of each of the isolated products. The PXRD patterns of the products obtained for each molar ratio are shown in Figure 3 together with the simulated PXRD patterns for **1** and **2** derived from the corresponding single-crystal X-ray analysis data. For a molar ratio in the range 1.0–5.0, the PXRD patterns of the respective products match well with the simulated pattern for isomer **1**, indicating that this is the only product formed in this region. When the ratio is in range 5.0–10, additional peaks were observed, that suggested the presence of a mixture of isomers **1** and **2**. On increasing the molar ratio above 10, the peaks for isomer **1** disappeared and only those for isomer **2** were then present. Thus, it can be concluded that as the content of $AgNO_3$ in the reaction solution increases, any existing isomer **1** is converted into isomer **2** with an associated conformational change of *m*-**L** from the "S"- to the "V"-shape as already discussed (Figure 1d and 2d). Hence,

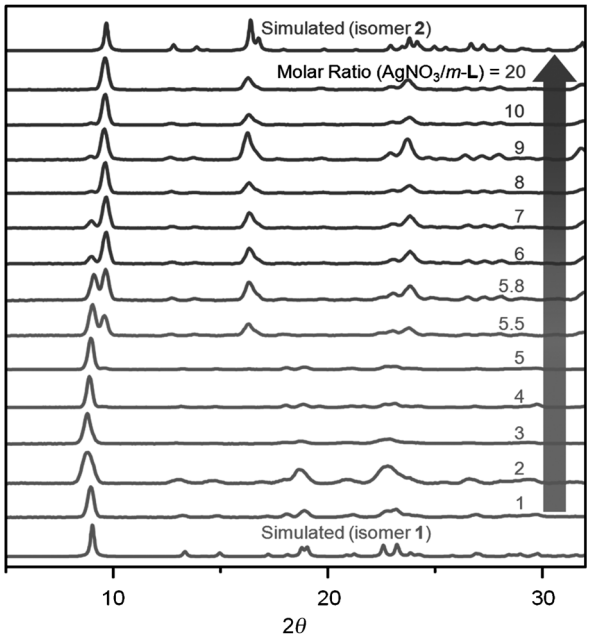

Figure 3. PXRD patterns of the products by varying the reactant mole ratios ($AgNO_3$/*m*-**L** = 1-20 equiv). Bottom and top data represent the simulated PXRD patterns of isomer **1** and isomer **2**, respectively, based on single-crystal X-ray analysis.

the combined approach of single-crystal X-ray analysis and PXRD pattern analysis has enabled in-depth information concerning the control of supramolecular isomerism through reactant molar ratio variation.

The reversibility between isomer **1** and isomer **2** were examined by analysing the recrystallised products with PXRD patterns (Figure S1 in the Supporting Information). When isomer **1** was immersed in a methanol containing 10–20 equivalents of $AgNO_3$ for 24 h, isomer **1** was maintained without change. On the other hand, when isomer **2** was immersed in a pure methanol solvent for 24 h, the conversion to isomer **1** by recrystallisation was confirmed. According to the observed irreversibility, it is concluded that isomer **1** with the "S"-shaped ligand conformation is thermodynamically more stable than isomer **2** with the "V"-shaped ligand conformation. The role of the excess amount of $AgNO_3$ on the conformational change is one of the core phenomena in this work. However, it is not easy to explain or predict such behaviour in the high concentrated electrolyte solution, because the ionic species act in a similar fashion as the solvent (medium effect).[13]

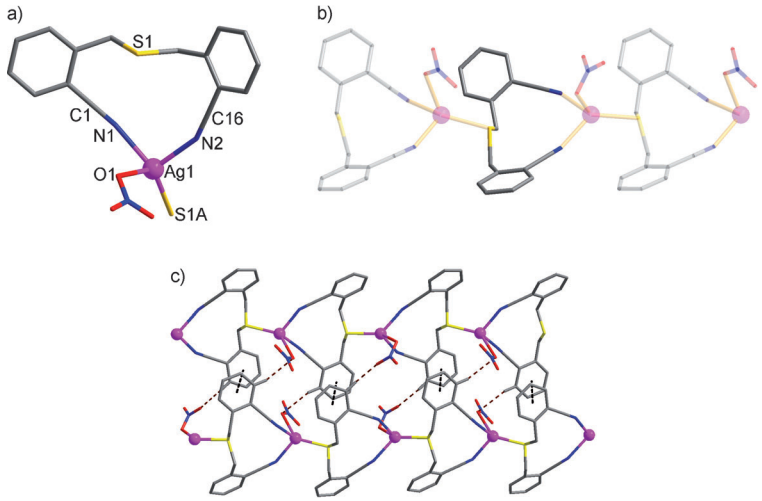

Figure 4. Crystal structure of **3**, $[Ag(o\text{-}\mathbf{L})NO_3]_n$: a) basic coordination unit, b) "C"-shaped ligand conformation in 1D looped chain, and c) interchain π–π interactions and C–H···O type hydrogen bonds.

Ag^I coordination polymers of *o*-L and *p*-L (3 and 4): In addition to the *m*-**L** complexes with $AgNO_3$ just discussed, the *ortho* (*o*-**L**) and *para* (*p*-**L**) ligands were also employed in a similar series of experiments in order to probe the possible molar-ratio dependency for these two ligand systems. As mentioned already, when the intrinsic coordination vectors for *o*-**L** and *p*-**L** are considered then metallocyclic and a linear complex product, respectively, might be expected to form. We found no dependence on the molar ratio of the reactants in each of these cases. This conclusion was also validated by the corresponding variable-molar-ratio PXRD patterns for these two ligand systems (Figure S2 in the Supporting Information).

Reaction of *o*-**L** with $AgNO_3$ afforded **3** as colourless crystals of formula $[Ag(o\text{-}\mathbf{L})NO_3]_n$. This product has an infinite 1D looped chain structure. Product **3** crystallised in the monoclinic space group $P2_1/c$ with $Z=4$. The asymmetric unit contains one molecule of *o*-**L**, one Ag atom, and one NO_3^-. The Ag atom is four-coordinate, being bound to two cyano nitrogen atoms from one *o*-**L** and one sulfur donor from an adjacent ligand to form the looped chain (Figure 4). The coordination sphere is completed by an O atom from NO_3^- bound in a monodentate manner (Ag1···O2 2.920(2) Å, Figure 4a). As anticipated, two cyano N atoms in *o*-**L** are linked by one μ_2-Ag atom through Ag–N bonds to form a metallocycle. The coordination geometry around Ag1 is distorted tetrahedral, with the "tetrahedral" angles falling in the range 78.53(6)–131.42(5)°. The large distortion is presumably largely caused by the formation of the 12-membered metallocycle incorporating a presumably rigid CN-Ag-NC bond angle. In the crystal packing (Figure 4c), each 1D loop-chain is aligned side by side and these interacts by the offset face-to-face π–π stacking; the intercentroid distance is 3.93 Å. C–H···O interchain hydrogen bonds are also present.

On reaction with $AgNO_3$, *p*-**L** forms the multichannel 3D framework **4** with the formula $[Ag_2(p\text{-}\mathbf{L})(NO_3)_2]_n$ (Figure 5). The product **4** crystallised in the monoclinic space group $C2/c$ with $Z=4$. The asymmetric unit contains a half-molecule of *p*-**L** located on a twofold axis, one Ag atom, and one NO_3^- ligand. The Ag atom is five-coordinate, being bound to one cyano nitrogen atom from one *p*-**L** and one sulfur atom of from another *p*-**L**. The coordination sphere is completed by three oxygen atoms from two nitrate anions, adopting mono- and bidentate bridging modes, respectively, that link two Ag centres (Ag1···Ag1B, 3.89 Å). Effectively, the two halves of each ligand connect two Ag atoms to generate a looped chain, with the sulfur nodes defining a helical arrangement (Figure 5b). The helix-like channels are further doubly connected by the nitrate ions, resulting in a 3D multichannel framework. Notably, the conformation of *p*-**L** has an elongated "M"-shape with its two cyano groups directed to opposite sides and being bound to Ag atoms in two neighbouring repeat units. Thus, the length of *p*-**L** in **4** (N1···N1C 14.44 Å) is much greater than that of *o*-**L** in **3** (N1···N2 3.50 Å).

It is notable that **4** features a 3D polymeric arrangement of formula $[Ag_2(p\text{-}\mathbf{L})(NO_3)_2]_n$. Even though its formula is similar to that of **1** and **2**, its structure differs markedly undoubtedly reflecting the preferred conformations of the respective ligand isomers.

In conclusion, three regioisomers of bis(cyanobenzyl)sulfide have been synthesised and their 1D and 3D silver(I) ni-

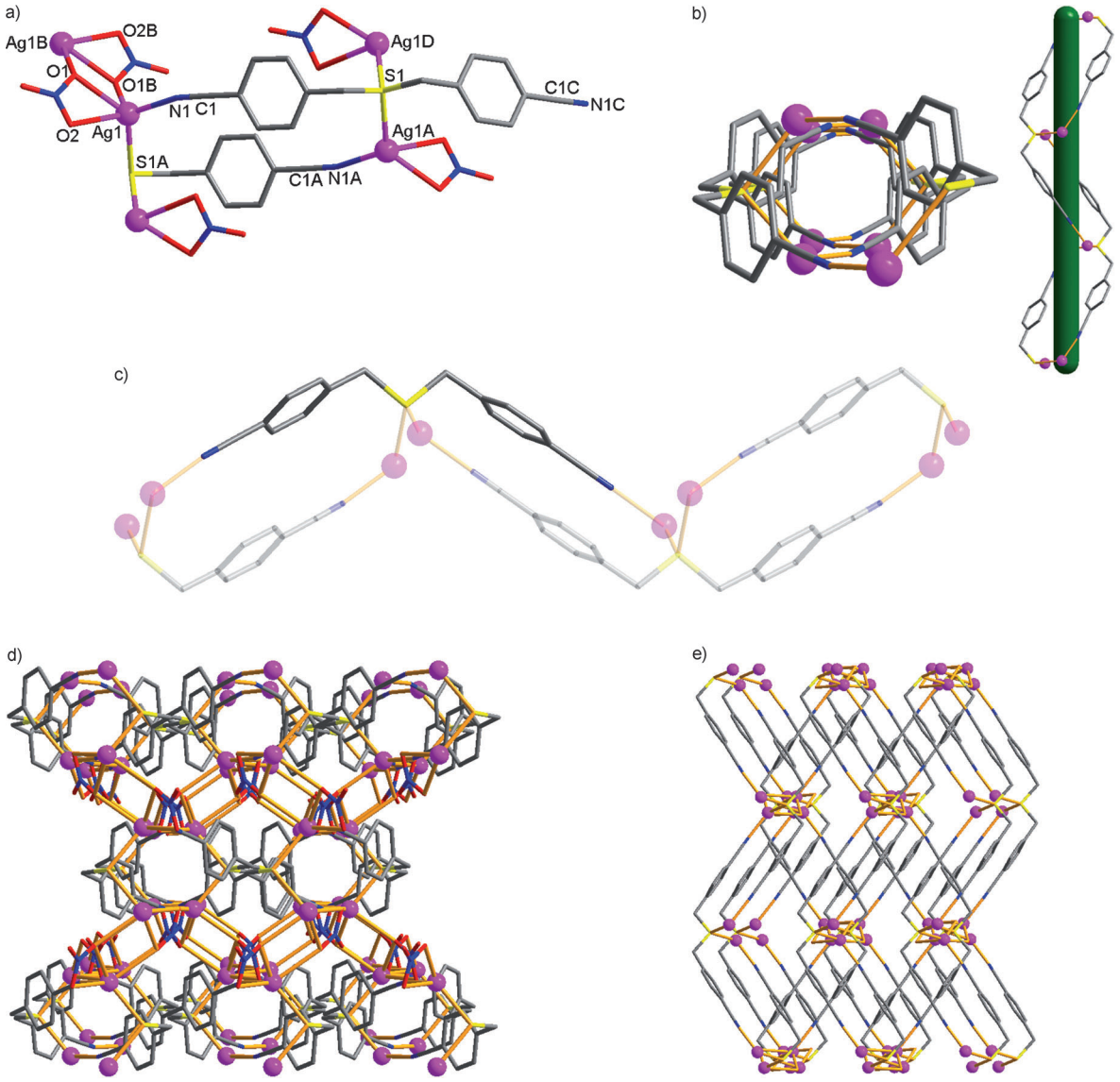

Figure 5. Crystal structure of **4**, $[Ag_2(p\text{-}\mathbf{L})(NO_3)_2]_n$: a) basic coordination unit, b) closer views of one channel unit of the multichannel type 3D structure (top view and side view), c) elongated "M"-shape ligand conformation, d) top view of the multichannel, and e) side view of the multichannel.

trate coordination polymers isolated and structurally characterised. Systematic investigation of these network complexes clearly shows that *m*-**L** gives rise to two 2D supramolecular isomers incorporating different conformations of the bound ligand. Formation of these isomers is dependent on the molar ratio of the reactants used for their synthesis. For *o*-**L** and *p*-**L**, however, variation of the metal-to-ligand ratio yielded identical products for each ligand across all molar ratios employed. The present study demonstrates that both the choice of particular semi-flexible ligand isomers of the present type as well as the variation of the molar ratio of reactants used for complex synthesis can each play an important role in influencing the structures of the corresponding frameworks generated in each case.

Experimental Section

General: All chemicals and solvents used in the syntheses were of reagent grade and were used without further purification. NMR spectra were recorded on a Bruker 300 spectrometer (300 MHz). The FT-IR spectra were measured with a Nicolet *i*S10 spectrometer. The ESI-mass spectra were obtained on a Thermo Scientific LCQ Fleet spectrometer. Each product obtained in this work was dried in a vacuum before elemental analysis, which was carried out on a Thermo Scientific Flash 2000 Series elemental analyser. Thermogravimetric analyses were recorded in a TA Instruments TGA-Q50 thermogravimetric analyser. Samples were heated at a constant rate of 5 °C min^{-1} from room temperature to 900 °C in a continuous-flow nitrogen atmosphere. The powder X-ray diffraction (PXRD) experiments were performed in a transmission mode with a Bruker GADDS diffractometer equipped with graphite monochromated $Cu_{K\alpha}$ radiation ($\lambda = 1.54073$ Å).

Synthesis and characterisation of *o*-L: A solution of Na_2S (0.6 g, 0.007 mol) in water (30 mL) was added to a stirred solution of 2-(bromome-

thyl)benzonitrile (3.0 g, 0.015 mol) in ethanol (45 mL) in a round-bottomed flask. The resulting solution was stirred at room temperature for 2 h, the ethanol was evaporated, and the residue was partitioned between water and dichloromethane. The combined organic layers were dried over anhydrous sodium sulfate and evaporated to dryness. The flash column chromatography (SiO_2; ethyl acetate/*n*-hexane 1:9) afforded the product as a pale-yellow solid in 60% yield. M.p. 115–116°C; ^{1}H NMR (300 MHz, $CDCl_3$): $\delta = 7.34$–7.65 (m, 8H; Ar), 3.91 ppm (s, 4H; ArCH_2S); ^{13}C NMR (75 MHz, $CDCl_3$): $\delta = 141.5$, 133.1, 133.0, 130.0, 127.8, 117.4, 112.7, 34.5 ppm; IR (KBr): $\tilde{\nu} = 3057$, 2969, 2936, 2233, 2222, 1594, 1490, 1473, 1446, 1402, 1300, 1247, 865, 770, 755, 704 cm^{-1}; MS (ESI): *m/z*: 287.15 $[C_{16}H_{12}N_2S_1+Na]^+$; elemental analysis calcd (%) for $C_{16}H_{12}N_2S_1$: C 72.70, H 4.58, N 10.60, S 12.13; found: C 72.86, H 4.51, N 10.84, S 12.30.

Synthesis and characterisation of *m*-L: The procedure was the same as for *o*-**L**, but with the use of 3-(bromomethyl)benzonitrile. The purification of the product, was also slightly different; it was recrystallised from dichloromethane/*n*-hexane (1:30). Yield: 65%; m.p. 103–104°C; ^{1}H NMR (300 MHz, $CDCl_3$): $\delta = 7.27$–7.57 (m, 8H; Ar), 3.63 ppm (s, 4H; ArCH_2S); ^{13}C NMR (75 MHz, $CDCl_3$): $\delta = 139.3$, 133.3, 132.3, 131.0, 129.4, 118.5, 112.8, 35.3 ppm; IR (KBr): $\tilde{\nu} = 3075$, 2934, 2228, 1595, 1577, 1478, 1429, 1418, 1225, 1083, 899, 825, 809, 728, 704, 684 cm^{-1}; MS (ESI): *m/z*: 287.08 $[C_{16}H_{12}N_2S_1+Na]^+$; elemental analysis calcd (%) for $C_{16}H_{12}N_2S_1$: C 72.70, H 4.58, N 10.60, S 12.13; found: C 72.84, H 4.55, N 10.88, S 12.35.

Synthesis and characterisation of *p*-L: The procedure was same as for *m*-**L**, but with the use of 4-(bromomethyl)benzonitrile; the synthesis of *p*-**L** has also been reported in the literature.[12] Yield: 60%. ^{13}C NMR (75 MHz, $CDCl_3$): $\delta = 143.2$, 132.5, 132.4, 129.7, 129.1, 118.6, 111.2, 35.5 ppm; IR (KBr): $\tilde{\nu} = 3051$, 3033, 2925, 2229, 1602, 1501, 1421, 1172, 1102, 915, 852, 809, 758, 1364, 1222, 1103, 1001, 801 cm^{-1}; MS (ESI): *m/z*: 287.17 $[C_{16}H_{12}N_2S_1+Na]^+$; elemental analysis calcd (%) for $C_{16}H_{12}N_2S_1$: C 72.70, H 4.58, N 10.60, S 12.13; found: C 72.84, H 4.55, N 10.88, S 12.32.

Preparation of 1, $[Ag_2(m\text{-}L)(NO_3)_2]_n$: Silver(I) nitrate (6.5 mg, 0.038 mmol) in methanol (2 mL) was added to a solution of *m*-**L** (10.0 mg, 0.038 mmol) in dichloromethane (2 mL). Slow evaporation of the solution afforded a colourless crystalline product **1** suitable for X-ray analysis. M.p. 194–196°C; IR (KBr pellet): $\tilde{\nu} = 3055$, 2936, 2250, 2231, 1599, 1578, 1480, 1298, 1137, 1084, 1033, 904, 832, 807, 746, 709 cm^{-1}; elemental analysis calcd (%) for $C_{16}H_{12}Ag_2N_4O_6S_1$: C 31.81, H 2.00, N 9.27, S 5.31; found: C 31.88, H 1.78, N 9.03, S 5.03.

Preparation of 2, $[Ag_2(m\text{-}L)(NO_3)_2]_n$: Silver(I) nitrate (64.5 mg, 0.76 mmol) in methanol (2 mL) was added to a solution of *m*-**L** (10.0 mg, 0.038 mmol) in dichloromethane (2 mL). Slow evaporation of the solution afforded a colourless crystalline product **2** suitable for X-ray analysis. M.p. 194–196°C; IR (KBr pellet): $\tilde{\nu} = 3076$, 2937, 2361, 2340, 2246, 2229, 1579, 1479, 1385, 1297, 1225, 1172, 1089, 1037, 899, 810, 703 cm^{-1}; elemental analysis calcd (%) for $C_{16}H_{12}Ag_2N_4O_6S_1$: C 31.81, H 2.00, N 9.27, S 5.31; found: C 31.91, H 1.94, N 9.28, S 5.61.

Preparation of 3, $[Ag(o\text{-}L)NO_3]_n$: Silver(I) nitrate (6.5 mg, 0.038 mmol) in methanol (2 mL) was added to a solution of *o*-**L** (10.0 mg, 0.038 mmol) in dichloromethane (2 mL). Slow evaporation of the solution afforded a colourless crystalline product **3** suitable for X-ray analysis. M.p. 169–171°C; IR (KBr pellet): $\tilde{\nu} = 3071$, 2978, 2242, 1596, 1487, 1452, 1382, 1322, 1304, 1241, 1159, 1036, 962, 828, 788, 768 cm^{-1}; elemental analysis calcd (%) for $C_{16}H_{12}AgN_3O_3S_1$: C 44.26, H 2.79, N 9.68, S 7.38; found: C 44.19, H 2.70, N 9.76, S 7.61.

Preparation of 4, $[Ag_2(p\text{-}L)(NO_3)_2]_n$: Silver(I) nitrate (6.5 mg, 0.038 mmol) in methanol (2 mL) was added to a solution of *p*-**L** (10.0 mg, 0.038 mmol) in dichloromethane (2 mL). Slow evaporation of the solution afforded a colourless crystalline product **4** suitable for X-ray analysis. M.p. 211–213°C; IR (KBr pellet): $\tilde{\nu} = 3035$, 2974, 2252, 2226, 1604, 1504, 1438, 1423, 1384, 1280, 1235, 1025, 869, 830, 812, 759 cm^{-1}; elemental analysis calcd (%) for $C_{16}H_{12}Ag_2N_4O_6S_1$: C 31.81, H 2.00, N 9.27, S 5.31; found: C 31.75, H 1.91, N 9.30, S 5.50.

X-ray crystallographic analysis: All data were collected on a Bruker SMART APEX II ULTRA diffractometer equipped with graphite monochromated $Mo_{K\alpha}$ radiation ($\lambda = 0.71073$ Å) generated by a rotating anode. The cell parameters for the compounds were obtained from a least-squares refinement of the spot (from 36 collected frames). Data collection, data reduction, and semi-empirical absorption correction were carried out using the software package of APEX2.[14] All of the calculations for the structure determination were carried out using the SHELXTL package.[15] In all cases, all non-hydrogen atoms were refined anisotropically and all hydrogen atoms were placed in idealised positions and refined isotropically in a riding manner along with the their respective parent atoms. Relevant crystal data collection and refinement data for the crystal structures of **1–4** are summarised in Table S1 in the Supporting Information. CCDC-943501 (**1**), CCDC-943502 (**2**), CCDC-943503 (**3**), and CCDC-943504 (**4**) contain the supplementary crystallographic data for this paper. These data can be obtained free of charge from The Cambridge Crystallographic Data Centre via www.ccdc.cam.ac.uk/data_request/cif.

Acknowledgements

This work was supported from NRF (2010-0022675 and 2012R1A4A1027750). E.L. acknowledges the support by NRF-2013-Fostering Core Leaders of the Future Basic Science Program.

Keywords: crystal engineering · isomers · networking · silver · supramolecular chemistry

[1] T. L. Hennigar, D. C. Macquarrie, P. Losier, R. D. Rogers, M. J. Zaworotko, *Angew. Chem.* **1997**, *109*, 1044–1046; *Angew. Chem. Int. Ed. Engl.* **1997**, *36*, 972–973.

[2] a) B. Moulton, M. J. Zaworotko, *Chem. Rev.* **2001**, *101*, 1629–1658; b) J.-P. Zhang, X.-C. Huang, X.-M. Chen, *Chem. Soc. Rev.* **2009**, *38*, 2385–2396; c) A. Y. Robin, K. M. Fromm, *Coord. Chem. Rev.* **2006**, *250*, 2127–2157.

[3] a) S. Masaoka, D. Tanaka, Y. Nakanishi, S. Kitagawa, *Angew. Chem.* **2004**, *116*, 2584–2588; *Angew. Chem. Int. Ed.* **2004**, *43*, 2530–2534; b) M.-L. Tong, S. Hu, J. Wang, S. Kitagawa, S. W. Ng, *Cryst. Growth Des.* **2005**, *5*, 837–839; c) P. Kanoo, K. L. Gurunatha, T. K. Maji, *Cryst. Growth Des.* **2009**, *9*, 4147–4156.

[4] a) T. H. Kim, J. Seo, K.-M. Park, S. S. Lee, J. Kim, *Inorg. Chem. Commun.* **2007**, *10*, 313–317; b) X. C. Huang, D. Li, X. M. Chen, *CrystEngComm* **2006**, *8*, 351–355; c) I. S. Lee, D. M. Shin, Y. K. Chung, *Chem. Eur. J.* **2004**, *10*, 3158–3165; d) X.-C. Huang, J.-P. Zhang, Y.-Y. Lina, X.-M. Chen, *Chem. Commun.* **2005**, 2232–2234; e) P. Cui, J. Wu, X. Zhao, D. Sun, L. Zhang, J. Guo, D. Sun, *Cryst. Growth Des.* **2011**, *11*, 5182–5187; f) P. A. Gale, M. E. Light, R. Quesada, *Chem. Commun.* **2005**, 5864–5866.

[5] a) J.-P. Zhang, S. Kitagawa, *J. Am. Chem. Soc.* **2008**, *130*, 907–917; b) Y. Jia, H. Li, Q. Guo, B. Zhao, Y. Zhao, H. Hou, Y. Fan, *Eur. J. Inorg. Chem.* **2012**, 3047–3053.

[6] a) I.-H. Park, S. S. Lee, J. J. Vittal, *Chem. Eur. J.* **2013**, *19*, 2695–2702; b) S. Aitipamula, A. Nangia, *Chem. Eur. J.* **2005**, *11*, 6727–6742.

[7] L. Fan, X. Zhang, Z. Sun, W. Zhang, Y. Ding, W. Fan, L. Sun, X. Zhao, H. Lei, *Cryst. Growth Des.* **2013**, *13*, 2462–2475.

[8] X. Bao, J.-L. Liu, J.-D. Leng, Z. Lin, M.-L. Tong, M. Nihei, H. Oshio, *Chem. Eur. J.* **2010**, *16*, 6169.
[9] Z.-M. Hao, X.-M. Zhang, *Cryst. Growth Des.* **2007**, *7*, 64–68.
[10] a) S. Park, S. Y. Lee, K.-M. Park, S. S. Lee, *Acc. Chem. Res.* **2012**, *45*, 391–403; b) H. J. Kim, L. F. Lindoy, S. S. Lee, *Cryst. Growth Des.* **2010**, *10*, 3850–3853; c) S. Park, S. Y. Lee, M. Jo, J. Y. Lee, S. S. Lee, *CrystEngComm* **2009**, *11*, 43–46; d) J. Seo, M. R. Song, J.-E. Lee, S. Y. Lee, I. Yoon, K.-M. Park, J. Kim, J. H. Jung, S. B. Park, S. S. Lee, *Inorg. Chem.* **2006**, *45*, 952–954; e) S. Y. Lee, J. Seo, I. Yoon, C.-S. Kim, K. S. Choi, J. S. Kim, S. S. Lee, *Eur. J. Inorg. Chem.* **2006**, 3525–3531.
[11] a) M. O. Awaleh, F. Baril-Robert, C. Reber, A. Badia, F. Brisse, *Inorg. Chem.* **2008**, *47*, 2964–2974; b) R. Peng, S.-P. Deng, M. Li, D. Li, Z.-Y. Li, *CrystEngComm* **2008**, *10*, 590–597.
[12] a) K.-M. Park, J. Seo, S.-H. Moon, S. S. Lee, *Cryst. Growth Des.* **2010**, *10*, 4148–4154; b) C. Barkenbus, E. B. Friedman, R. K. Flege, *J. Am. Chem. Soc.* **1927**, *49*, 2549–2553; c) Y. W. Park, Y. Na, D.-J. Baek, *Bull. Korean Chem. Soc.* **2006**, *27*, 2023–2027.
[13] H. S. Harned, B. B. Owen, *The Physical Chemistry of Electrolyte Solutions*, Reinhold, New York, USA **1958**.
[14] APEX2 Version 2009.1-0 Data collection and Processing Software, Bruker AXS Inc., Madison, Wisconsin, USA **2008**.
[15] SHELXTL-PC Version 6.22: Program for Solution and Refinement of Crystal Structures, Bruker AXS Inc., Madison, Wisconsin, USA **2001**.

Received: July 7, 2013
Published online: ■■ ▮▮, 0000

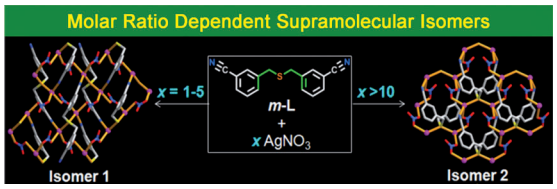

The ratio is the key: On varying the molar ratio of the reactants, $AgNO_3$ and tridentate *m*-**L** ligand, supramolecular isomers **1** and **2** comprising a 2D polymeric network were obtained. Conformational differences of *m*-**L** play a crucial role in the 2D network structures adopted for isomers **1** and **2**.

Supramolecular Chemistry

*E. Lee, J.-Y. Kim, S. S. Lee,**
*K.-M. Park** ..... ■■■■–■■■■

Molar-Ratio-Dependent Supramolecular Isomerism: Ag^I Coordination Polymers with Bis(cyanobenzyl)sulfides

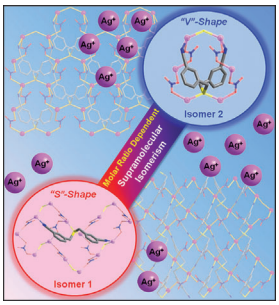

Supramolecular Isomerism

Silver supramolecular isomers **1** and **2** each comprising a 2D polymeric coordination network were obtained on varying the molar ratio of the reactants (silver and a ligand based on bis(cyanobenzyl)sulfide). Notably, the overall structural motifs of **1** and **2** are mainly due to the conformational variation of the ligand: "S"-shaped in **1** and "V"-shaped in **2**. More details of this interesting supramolecular isomerism are given by S. S. Lee, K.-M. Park et al. in their Communication on page ■■ ff.